Pauli blocking in three-body models of halo nuclei

I. J. Thompson
Department of Physics, University of Surrey, Guildford GU2 5XH, United Kingdom

B. V. Danilin and V. D. Efros
The Kurchatov Institute, 123182 Moscow, Russia

J. S. Vaagen
SENTEF, Institute of Physics, University of Bergen, Norway
and NORDITA, Blegdamsvej 17, DK-2100 Copenhagen Ø, Denmark

J. M. Bang
Niels Bohr Institute, Blegdamsvej 17, DK-2100 Copenhagen Ø, Denmark

M. V. Zhukov
Department of Physics, Chalmers University of Technology and Göteborg University, Göteborg, Sweden
(Received 24 March 1999; published 21 January 2000)

In three-body models of halo nuclei such as ^{6}He, Pauli blocking is needed to remove components of the halo wave function that would disappear under full antisymmetrization. We compare a full projection-operator method with two others presently used for the purpose. A range of differences is found, small for bound states and resonances but larger for nonresonant continuum states. We indicate discriminating characteristics sensitive to the off-shell behavior.

PACS number(s): 21.60.Gx, 21.10.Pc, 21.45.+v, 25.60.Gc

I. INTRODUCTION

Recent progress in the theory of halo nuclei has led to more accurate models of the ground state of ^{6}He and of its breakup continuum states. Our previous investigations of $A=6$ nuclei [1–10] and ^{11}Li [11,12], and also those of other authors [13–26] using a variety of methods, have shown that numerous characteristics of the *discrete* states of the halo nuclei can be accounted for by using three-body dynamics with ''fundamental'' pairwise interaction potentials supplemented by weak three-body potentials.

The three-nucleon problem has been studied for its sensitivity to the off-shell behavior of its interactions. In more complicated systems, the best known stable nucleus is ^{6}Li, with neutron- and proton-rich neighbors ^{6}He and ^{6}Be, all of which have a dominant $\alpha+N+N$ structure. The previous attempts to compare local and nonlocal Pauli treatments in the integral equation method [27], or with a combination of coordinate-space Faddeev equations and hyperharmonics methods [1,3,28], came to the conclusion that for a wide class of electromagnetic and geometrical observables for both bound and quasibound states, various Pauli treatments give very similar results. We will examine below whether scattering observables are more sensitive indicators of the differences between the alternative Pauli methods.

The developments of dynamic approaches to the three-body continuum theory [1,14,17,24,29–31] make it now possible to investigate also the unbound states of these nuclei that are populated in breakup reactions. The previously known spectrum of ^{6}He contained only the 0^+ bound state and the well-known 2^+ ($E^*=1.8$ MeV) three-body resonance [32], but our recent models [10,9] predict new states in the three-body $\alpha+n+n$ continuum below the ^{3}H+^{3}H threshold at about 13 MeV. The unusually large electromagnetic dissociation (EMD) cross section for ^{11}Li and ^{6}He projectiles, as well as for other neutron dripline nuclei [33–35], has revealed an enhanced dipole breakup strength for these halo nuclei. While for ^{11}Li an $\mathcal{E}1$ response (''strength'') function has been reconstructed from exclusive experiments [36,37], such information has only very recently been obtained [38] for ^{6}He. Angular distributions and angular correlations are now being measured [39,38], supplementing the previous measurements of momentum distributions from fragmentation [40–44] and the limited data from charge-exchange reactions with ^{6}Li to the ^{6}He continuum [45–47].

With increased accuracy of calculations and of experiments involving ^{6}He, it has become necessary to reexamine how the $A=6$ system has been projected onto a three-body model space. Of special interest here is the question of Pauli blocking, arising because the neutron-core interactions have deeply bound eigenstates which must be regarded as already occupied by core nucleons, and blocked to the halo neutrons.

Pauli blocking is needed to remove components of the halo wave function that would disappear under full antisymmetrization. We compare a full projection-operator method with others recently proposed: either using repulsive potentials in those neutron-core partial waves with bound states or by removing the lowest-energy eigensurface in a hyperspherical adiabatic approximation. These alternatives give Pauli effects which are local in some coordinate, but their accuracy needs to be checked not only for bound states [21,26] but also for resonant and nonresonant scattering.

Particular theoretical attention has been focused on the mechanism for the large EMD cross section, namely, the

electric dipole excitation to the continuum. There has been a search for a low-lying ''soft dipole resonance'' ([48–50,41,51,52,6,38], and references therein), where the two halo nucleons are envisaged to oscillate with respect to the core, which carries the charge. The $B(\mathcal{E}1)$ strength function to dipole states in ^{6}He will turn out to be particularly sensitive to the Pauli treatment, since the negative parity of the dipole states means that they probe the *s*-wave channels of n-α relative motion: exactly those channels where there are occupied bound states.

We will examine the bound and continuum states in the method of hyperspherical harmonics (HH) expansions. This allows the long-range behavior of the three-body wave functions to be explicitly calculated, and hence avoids the theoretical shortcomings in analyses within the random phase approximation (RPA) (mean field) method, which treat the three-body continuum (most relevant for these Borromean systems) in a rather approximate way, or else in the frame of two-body (cluster) dynamics. The complex rotation method has been applied to the three-body Schrödinger equation [17], or to the three-body resonating group method (RGM) [14], but enables one only to calculate the parameters of three-body resonant states—their widths, positions, and partial content. No theoretical paper (except for [24]) has predicted a low-lying 1^- resonance in ^{6}He, so it may well be that the dipole continuum is nonresonant, but still enhanced for dynamical reasons. More experimental information is needed to clarify this question.

The structure of this paper is as follows. In Sec. II we summarize the theoretical framework necessary to treat the ground state and continuum structure of halo nuclei with three-body dynamical models. Section II B discusses the different methods proposed for treating Pauli blocking, and in Sec. III we present the physical inputs for and results of three-body calculations for ^{6}He, using the various Pauli treatments. Pauli effects in the $\alpha+n+n$ continuum are discussed in Sec. IV, and conclusions are given in Sec. V.

II. THEORY

Cluster models of light nuclei allow us to approximate the many-nucleon problem by a few-body one, and for the treatment of the latter problem a number of methods have been developed. Faddeev [53,18] and Schrödinger few-body formulations have been successfully solved with the help of momentum space [18], variational [19,15], and hyperspherical harmonic [3] procedures. Faddeev equations have also been solved with the adiabatic hyperspherical [28] method. For potentials with strongly repulsive cores, an approach such as the correlated hyperspherical method of [54,55] would become appropriate.

In the RGM [14,16,22,25] and the generator-coordinate method (GCM) [20] the composite structure of clusters manifests itself through non-local exchange integral kernels. The orthogonality condition model [56], derived from the RGM, reduces the complicated Hill-Wheeler equation to a Schrödinger one with a physically transparent projecting out of Pauli-blocked states from the spectrum of the binary Hamiltonian. An alternative method, generating a spectrally equivalent Hamiltonian, is to use the double supersymmetric transform [57–62]. Both approaches give the same on-shell behavior, but are different off shell, which can be critical in the three-body situation. We will see below examples of such differences.

A. Three-body hyperspherical basis

Given particle positions $\mathbf{R}_1$ and $\mathbf{R}_2$ for the neutrons and $\mathbf{R}_3$ for the core, the standard [9] translationally invariant normalized sets of Jacobi coordinates $\mathbf{x}$ and $\mathbf{y}$ are defined using the mass ratios $A_i=m_i/m$ (for m a unit nucleon mass), as follows:

$$\mathbf{x}=(A_{12})^{1/2}\mathbf{r}_{12}=(A_{12})^{1/2}(\mathbf{R}_2-\mathbf{R}_1),$$

$$\mathbf{y}=(A_{(12)3})^{1/2}\mathbf{r}_{(12)3}$$
$$=(A_{(12)3})^{1/2}[\mathbf{R}_3-(A_1\mathbf{R}_1+A_2\mathbf{R}_2)/(A_1+A_2)], \quad (1)$$

$$\mathbf{R}=(A_1\mathbf{R}_1+A_2\mathbf{R}_2+A_3\mathbf{R}_3)/A.$$

Here A_{12} and $A_{(12)3}$ are the appropriate reduced masses. We use hyperspherical coordinates ρ, α, $\hat{\mathbf{x}}$, and $\hat{\mathbf{y}}$, where $\rho=(x^2+y^2)^{1/2}$ is the hyperradius and $\alpha=\arctan(x/y)$ is the hyperangle.

The choice of $\mathbf{x}$ and $\mathbf{y}$ simplifies the antisymmetrization of the wave function between the two neutrons: when constructing the channels in this basis, the antisymmetrization can be included by imposing $\{l_x+S+T=\text{odd}\}$, where l_x is the relative orbital angular momentum between the two neutrons, and S and $T=1$ are the total spin and isospin of the two-neutron subsystem.

We seek our bound-state and continuum wave functions in the form of an expansion using hyperspherical harmonic basis functions:

$$\Upsilon^{l_x l_y}_{JKLSM}(\Omega_5)=[\mathcal{Y}^{l_x l_y}_{KLM}(\Omega_5)\otimes X_S]_{JM}, \quad (2)$$

with

$$\mathcal{Y}^{l_x l_y}_{KLM}(\Omega_5)=\psi^{l_x\,l_y}_K(\alpha)[Y_{l_x}(\hat{\mathbf{x}})\otimes Y_{l_y}(\hat{\mathbf{y}})]_{LM}. \quad (3)$$

The quantum number K is called the hypermomentum. These $\mathcal{Y}^{l_x l_y}_{KLM}(\Omega_5)$ are called ''hyperspherical harmonics.'' Here the $\alpha,\theta_x,\phi_x,\theta_y$, and ϕ_y variables are denoted collectively by Ω_5, the notation $[\cdots]$ indicates tensor coupling, and X_S is a spin function. Other quantum numbers are the Jacobi orbital momenta l_x and l_y, and the total orbital momentum L and its projection M. The hyperangular part of the HH (depending on α) has the following explicit form:

$$\psi^{l_x l_y}_K(\alpha)=N^{l_x l_y}_K(\sin\alpha)^{l_x}(\cos\alpha)^{l_y}P^{l_x+1/2,l_y+1/2}_{(K-l_x-l_y)/2}(\cos 2\alpha), \quad (4)$$

where $P^{\alpha,\beta}_n$ are Jacobi polynomials and $N^{l_x l_y}_K$ is a normalization factor (see, e.g., [3]).

We look for three-body wave functions of the form

$$\Psi^T_{JM}(\mathbf{x},\mathbf{y}) = \rho^{-5/2} \sum_{KLSl_x l_y} \chi^{LS}_{Kl_x l_y}(\rho) \Upsilon^{l_x l_y}_{JKLSM}(\Omega_5) X_{TM_T}, \tag{5}$$

with hyperradial wave functions $\chi^{LS}_{Kl_x l_y}(\rho)$ that satisfy either bound-state

$$\chi_{K\gamma}(0) = 0, \quad \chi_{K\gamma}(\rho \to \infty) \sim \exp(-\kappa\rho) \tag{6}$$

(where $\gamma = \{l_x, l_y, L, S\}$, $\mathcal{L} = K + 3/2$, and $\kappa = \sqrt{2m|E|/\hbar^2}$) or scattering

$$\chi_{K\gamma,K'\gamma'}(\kappa\rho) \sim H^-_{K+3/2}(\kappa\rho)\,\delta_{K\gamma,K'\gamma'} - S_{K\gamma,K'\gamma'} H^+_{K+3/2}(\kappa\rho) \tag{7}$$

boundary conditions according to the three-body energy E. These particularly simple boundary conditions are satisfied for Borromean systems, as no two-body bound states exist asymptotically.

In this basis, the partial-wave coupling interactions are the matrix elements

$$V_{K'\gamma',K\gamma}(\rho) = \langle \Upsilon_{K\gamma}(\Omega_5) | V_{12} + V_{13} + V_{23} + V_{123} | \Upsilon_{K'\gamma'}(\Omega_5) \rangle, \tag{8}$$

where V_{ij} is the interaction between bodies i and j, and V_{123} is a possible three-body force to be discussed later.

In the case of short-range pairwise particle interactions the three-body mean field behaves at large ρ values as $V_{K\gamma,K'\gamma'}(\rho \to \infty) \sim \rho^{-n}$ with $n \geqslant 3$ $(n \geqslant l_x + l'_x + 3)$. This power law decrease, obtained for finite-range pairwise potentials V_{ij}, reflects the possibility of two particles interacting when far away from the third particle.

With local potentials, the wave function Ψ^T_{JM} would be a solution to the Schrödinger three-body equation

$$(T + V_{12} + V_{13} + V_{23} + V_{123} - E)\Psi^T_{JM} = 0. \tag{9}$$

After projecting onto the hyperangular parts of the wave function we would obtain a set of coupled equations:

$$\left(-\frac{\hbar^2}{2m}\left[\frac{d^2}{d\rho^2} - \frac{\mathcal{L}(\mathcal{L}+1)}{\rho^2} \right] - E \right) \chi_{K\gamma}(\rho) + \sum_{K'\gamma'} V_{K'\gamma',K\gamma}(\rho)\ \chi_{K'\gamma'}(\rho) = 0. \tag{10}$$

As it stands, however, this coupled equation set does not take any account of Pauli blocking.

B. Pauli blocking

In the present approach, we wish to start with the standard kinds of local potentials V_{ij} which have proved successful in many branches of nuclear physics, and seek to use them as ''fundamental interactions'' with minimum modification within three-body models. We have still, however, to consider the effects of antisymmetrization, the existence of ''forbidden states'' in the cluster-cluster motion, and the possibility of l dependence of the interactions.

In general, antisymmetrization of the full A-body wave function leads to exchange terms which are nonlocal in the cluster-cluster relative coordinates, and these nonlocalities lead to l dependence of the local phase-equivalent potentials [63,64]. We can therefore use different potential strengths in different partial waves. This, in any case, is often necessary as our local potentials are fitted to the experimental phase shifts for binary scattering and to any bound states or resonances in that two-body channel.

Even when the two-body bound and scattering states are reproduced, the three-body situation requires the Pauli principle to be considered again. This is because the interactions typically have negative energy eigenstates which must be taken as already ''occupied'' in one of the composite bodies. Two-body scattering states are automatically orthogonal to these, if a fixed Hamiltonian is used, but in the three-body case of a core and two neutrons, the additional nn interaction could scatter one of the neutrons into one of the core occupied states.

The three-body case therefore requires some treatment of antisymmetrization, at the very least a Pauli blocking constraint to forbid the valence neutrons entering the occupied core states. Different approximations to the complete antisymmetric approach have therefore been suggested to construct treatable interactions for use in three-body models.

PP: When the effective intercluster interactions are sufficiently deep to produce bound binary states which would be eliminated by full antisymmetrization, these occupied states should be projected out as Pauli forbidden. We should solve the Schrödinger equation for the three-body wave functions within the allowed (sub)space, not merely project out forbidden states after finding a solution. The projection can be done by the pseudopotential method [19,65,66] or directly by means of projection operators [67–69].

PS: By using a supersymmetric transform [57–59,61,62] of the n-core potential. For a potential having a forbidden state, we can obtain a spectrally equivalent potential without this state but with a characteristic r^{-2} repulsive singularity at the origin.

PC: Since phase shifts for most of the cluster scattering are defined in a finite energy range, it is possible to introduce an auxiliary repulsive interaction (a soft ''Pauli core'') in the same partial components of effective intercluster interactions where forbidden states are expected, and fit these interactions to the experimental phase shifts.

PA: For large hyperradius ρ, the coupling matrix $V_{K'\gamma',K\gamma}(\rho)$ has a set of negative-energy eigenvalues which are the states to be blocked. These can be projected out, for each ρ separately, as in Refs. [21,24], and a revised coupling matrix $\hat{V}_{K'\gamma',K\gamma}(\rho)$ constructed.

Ignoring the Pauli principle completely is obviously incorrect for ground states, but may be considered in scattering problems, so some results from this assumption will be presented below for resonances (we will refer to this method as ''NO PP'').

The PP and PA methods construct projection operators P (local in ρ in the PA case) to remove unwanted eigensolutions. Their effect may be generically formulated as finding the eigenenergies e and eigenvectors c_e of a matrix $\mathbf{A}$ in an

allowed subspace $Pc_e=0$. This is accomplished, given the matrix **A**, by solving

$$(1-P)\mathbf{A}(1-P)c_e+E_0Pc_e=ec_e. \tag{11}$$

Here, E_0 is a large positive energy (1000 MeV) to which the forbidden eigenstates are moved, to avoid contamination of the halo states of interest near the breakup threshold. All the solutions of Eq. (11) with $e\neq E_0$ satisfy $Pc_e=0$. In the PA method, the couplings themselves are modified by $\hat{V}(\rho)=[1-P(\rho)]V(\rho)[1-P(\rho)]+E_0P(\rho)$.

All these methods of including antisymmetrization effects essentially coincide on the two-body energy shell and asymptotically at large hyperradius in the three-body situation. A peculiarity of three-body dynamics, however, is its sensitivity to off-shell behavior of pair interactions, enabling us in principle to discriminate between the different classes of interactions. The results for methods PP and PC have already been compared for bound states of ^{6}Li [18] and ^{6}He [3], and the results of PP and PS have been compared for ^{6}He, ^{11}Li, and ^{14}Be [62]. They were found to be almost coinciding for many properties of the ground state. Later we will examine the differences which arise for resonant and nonresonant continuum states. Thus the three-body continuum gives us what may be unique possibility to investigate the consequences of these differences in approach.

C. Solution of the coupled HH equations

We have in the PC and PS cases to solve the set of N coupled equations [Eq. (10)], while in the PP method there will be orthogonality conditions $\langle u_n|\psi\rangle=0$, with u_n the wave functions of occupied states in the binary subsystems. The PA method solves Eq. (10) with modified local couplings $\hat{V}$. For Borromean systems, the hyperradial wave functions $\psi_{K\gamma}(\rho)$ for bound states have, for uncharged particles, the standard boundary conditions of decaying exponentially at large distances, while the continuum wave functions become a linear combination of Hankel functions. The scattering boundary conditions describe the in- and outgoing three-body spherical waves, so that $S_{K\gamma,K_0\gamma_0}$ is the S matrix for the $3\rightarrow3$ scattering for an incoming wave in channel $K_0\gamma_0$. We only deal with Borromean (or democratic) types of three-body problems, where there are no two-body bound states in the asymptotic regions.

To solve the coupled equations [Eq. (10)], we previously [1,3,4,6] integrated N linearly independent solutions from $\rho=0$ to $\rho=\rho_m$, for some radius ρ_m beyond which the couplings $V_{K'\gamma',K\gamma}(\rho)$ are assumed to be negligible. A linear combination of these solutions was then found, in order to satisfy the appropriate boundary conditions. This was straightforward for limited numbers of channels (N up to 10 or 12), but for larger sets the solutions become linearly dependent. This is because the large range of centrifugal barriers $\mathcal{L}(\mathcal{L}+1)/\rho^2$ means that some channels are, for a large period, being integrated in their classically forbidden domain, and (as discussed in [70]) the linear independence of the exponentially decreasing solutions is lost. This method, moreover, does not easily enable the PP Pauli method.

1. R-matrix method

To avoid numerical instabilities with large sets, we use an expansion on Sturmian or Sturmian-like radial basis functions. For bound-state wave functions, it is convenient to use Sturmian states, which are eigenstates at a fixed energy for varying multiples of some diagonal potential. This has been developed for bound states in deformed nuclei [71,72], and we have also found the method to be useful for hyperradial bound states [73]. For scattering states, however, the Sturmian states are not suitable as they have few oscillations at large distances up to ρ_m. We therefore follow standard R-matrix methods, and use a basis set of ''energy eigenstates'' of the diagonal terms of Eqs. (10):

$$\left(-\frac{\hbar^2}{2m}\left[\frac{d^2}{d\rho^2}+\frac{\mathcal{L}(\mathcal{L}+1)}{\rho^2}\right]+V_{K\gamma,K\gamma}(\rho)-\alpha_q\right)f^q_{K\gamma}(\rho)=0 \tag{12}$$

for eigenenergies α_q, with the basis functions all having fixed logarithmic derivatives $\beta=d\ln f^q_{K\gamma}(\rho)/d\rho$ at ρ_m. The constancy of the logarithmic derivatives β means that (for each $K\gamma$ channel separately) the $f^q_{K\gamma}$ form an orthogonal basis set over the interval $[0,\rho_m]$, and *over this range* they can be normalized to unity. Then, as many $q=1,\ldots,Q$ of the orthonormal $f^q_{K\gamma}$ per $K\gamma$ channel can be used as desired for accuracy. For $\beta<0$ the basis states with low $\alpha_q<0$ will be similar to the Sturmian states with low potential multipliers, and hence suitable for bound state expansions. Higher $\alpha_q>0$ basis states will oscillate out to ρ_m, and can be used in expansions of continuum states.

The wave functions of the coupled problem (10) can now be solved completely over the interior range $[0,\rho_m]$, by using the orthonormal basis set of the $\{f^q_{K\gamma}(\rho)\}$ with coefficients to be determined. The coefficients are found in two stages: first by finding all the eigensolutions $\phi^p_{K\gamma}(\rho)$ of Eq. (10) using the above orthonormal basis, and then expanding the scattering wave functions in terms of these $\phi^p_{K\gamma}(\rho)$.

The first stage, the diagonalization of interior Schrödinger equation (10) yields $P=QN$ eigenenergies e_p with corresponding multichannel eigenstates

$$\phi^p_{K\gamma}(\rho)=\sum_{q=1}^{Q} c^{pq}_{K\gamma}f^q_{K\gamma}(\rho). \tag{13}$$

Eigenstates here with $e_p<0$ are close to the bound states, while solutions with $e_p>0$ contribute to the scattering solutions. Certain of the $e_p>0$ solutions may correspond to low-lying resonances if those are present, but the majority of the positive eigenenergies have no simple physical interpretation. These $\phi^p_{K\gamma}(\rho)$ form of course another orthonormal basis in the interior region.

For scattering states at arbitrary energy E with incoming waves in channel $K_0\gamma_0$, the coupled solutions are then expanded in terms of the multichannel eigenstates as $\psi_{K\gamma:K_0\gamma_0}=\Sigma_p A^p_{K_0\gamma_0}\phi^p_{K\gamma}$. If we define an R matrix at energy E by

$$\psi_{K\gamma:K_0\gamma_0}(\rho)=\sum_{K'\gamma'} R_{K\gamma:K'\gamma'}(E)\left[\frac{d}{d\rho}\psi_{K'\gamma':K_0\gamma_0}(\rho) - \beta\psi_{K'\gamma':K_0\gamma_0}(\rho)\right] \tag{14}$$

in the limit of $\rho\to\rho_m$ from above, then the R matrix $\mathbf{R}$ can be calculated directly from the eigenstates by standard methods [74]:

$$R_{K\gamma:K'\gamma'}(E)=\frac{\hbar^2}{2m}\sum_{p=1}^{P}\frac{\phi^p_{K\gamma}(\rho_m)\phi^p_{K'\gamma'}(\rho_m)}{e_p-E}. \tag{15}$$

The R matrix calculated by Eq. (15) is only exact when the sum over p extends to all energies e_p. To improve the accuracy of calculations with finite Q and P, the Buttle correction [75] is added to the diagonal terms of this expression. Using Eq. (14), the scattering S matrix is given in terms of $\mathbf{R}$ by

$$\mathbf{S}=[\mathbf{H}^+-\mathbf{R}(\mathbf{H}'^+-\beta\mathbf{H}^+)]^{-1}[\mathbf{H}^--\mathbf{R}(\mathbf{H}'^--\beta\mathbf{H}^-)] \tag{16}$$

and the expansion coefficients for the wave functions are

$$A^p_{K_0\gamma_0}=-\frac{\hbar^2}{2m}\frac{1}{e_p-E}\sum_{K'\gamma'}\phi^p_{K'\gamma'}(\rho_m) \times\{\delta_{K'\gamma',K_0\gamma_0}[H'_{\mathcal{L}'}(\kappa\rho_m)-\beta H^-_{\mathcal{L}'}(\kappa\rho_m)] - S_{K'\gamma',K_0\gamma_0}[H'_{\mathcal{L}'}(\kappa\rho_m)-\beta H^+_{\mathcal{L}'}(\kappa\rho_m)]\}. \tag{17}$$

For short-range potentials, we can choose ρ_m outside the range of the couplings, and the Hankel functions $\mathbf{H}^{\pm}$ are diagonal matrices. The calculations in Ref. [9] made this approximation. Since, however, we know that the couplings of Eq. (8) have long-range ρ^{-3} behavior, this necessitates a proper treatment of couplings in the asymptotic region. We therefore use the Light-Walker methods of [76] to propagate the R matrix from ρ_m out to some larger radius ρ_a where Gailitis expansions [77] converge. This effectively includes all couplings out to infinite ρ, and avoids the effects of artificial poles [78].

The coefficients $c^{pq}_{K\gamma}$ and energies e_p in Eq. (13) satisfy matrix equations

$$\alpha_q c^{pq}_{K\gamma}+\sum_{q'K'\gamma'}\langle f^q_{K\gamma}|V_{K\gamma,K'\gamma'}|f^{q'}_{K'\gamma'}\rangle c^{pq'}_{K'\gamma'}=e_p c^{pq}_{K\gamma} \tag{18}$$

for each eigenstate p, which are of the matrix form

$$\mathbf{A}c=ec. \tag{19}$$

2. Projection operators

The projection operators P of the PP method can be constructed as follows. In addition to the set (1) of Jacobi coordinates we shall use the two other scaled sets

$$\mathbf{x}_i=(A_{i3})^{1/2}\mathbf{r}_{i3},\quad \mathbf{y}_i=(A_{(i3)j})^{1/2}\mathbf{r}_{(i3)j},$$

for $i=1,2$ and cyclic i, j, k. The two-body forbidden states are of the form $u_m(\mathbf{x}_i)$, and the subspace of functions Ψ, in which the Schrödinger equation is solved, is obtained from the total space by imposing the orthogonality conditions

$$\int d\mathbf{x}_i\, u_m(\mathbf{x}_i)^*\Psi=0. \tag{20}$$

The integration in Eq. (20) proceeds at fixed $\mathbf{y}_i$. It is convenient to replace the conditions (20) by the set of equivalent three-body orthogonality conditions $\langle U^i_{mn}|\Psi\rangle=0$ where $U^i_{mn}(\mathbf{x}_i,\mathbf{y}_i)=u_m(\mathbf{x}_i)s_n(\mathbf{y}_i)$, and $s_n(\mathbf{y})$ is a complete set of spline functions as used in [67] and [9].

Thus the three-body Pauli-forbidden states are just the linear combinations

$$\sum_i\sum_{m,n}c^i_{mn}U^i_{mn} \tag{21}$$

and the projection operator is

$$P=\sum_\lambda|\overline{U}_\lambda\rangle\langle\overline{U}_\lambda|, \tag{22}$$

where $\overline{U}_\lambda$ are orthonormalized basis states spanning the subspace (21). The subspace (21) consists of states symmetric and antisymmetric with respect to neutron permutations. Only the latter states are of interest for us, and the operator (22) is taken in the subspace of such states.

In the framework of the R-matrix method of the preceding section the operator (22) is obtained as follows. The wave function $U_{mn}(\mathbf{x},\mathbf{y})$ (for total spin state $|JM\rangle$) is expanded in the hyperspherical basis $f^q_{K\gamma}(\rho)$ as

$$U_{mn}(\mathbf{x},\mathbf{y})=\sum_{K\gamma q}w^q_{mnK\gamma}f^q_{K\gamma}(\rho)\Upsilon^{l_xl_y}_{JKLSM}(\Omega_5), \tag{23}$$

where $\gamma=\{l_x,l_y,L,S\}$ as before. The orthogonality requirement of $\langle u_m(\mathbf{x})|\psi_{K\gamma:K_0\gamma_0}\rangle=0$ is now satisfied by requiring that each interior multichannel eigenstate p has no forbidden component:

$$\sum_{qK\gamma}w^q_{mnK\gamma}c^{pq}_{K\gamma}=0 \tag{24}$$

for each forbidden state m, each spline function n. In matrix form, this is $\langle w_{mn}|c\rangle=0$ for each eigenstate p. We therefore construct a projection operator

$$P=\sum_{mn}|\tilde{w}_{mn}\rangle\langle\tilde{w}_{mn}|, \tag{25}$$

where the set $\{\tilde{w}_{mn}\}$ is an orthonormalized basis set constructed by the Gramm-Schmidt process from the $\{w_{mn}\}$.

We now diagonalize in the *allowed subspace* of $Pc=0$, and ensure this by *replacing* matrix equations (19) by an equation of the form (11). In this way, both the bound state

and continuum wave functions can be made orthogonal to the required set of occupied core states.

D. Dipole response distribution

The electromagnetic dipole operator for transitions to the continuum is

$$T^{\mathcal{E}}_{1m}=\sum_i eZ_i r_i Y_{1m}(\hat{r}_i)=\sqrt{\frac{3}{4\pi}}\sum_i eD_{im}, \qquad (26)$$

where $\mathbf{r}_i=\mathbf{R}_i-\mathbf{R}$ is the distance of particle i from the center of mass of the whole nucleus, and $\mathbf{D}_i=Z_i\mathbf{r}_i$. For the present halo nuclei, the only charged particle is the core ($i=3$), with $\mathbf{r}_3=\sqrt{A_{12}/(AA_3)}\mathbf{y}$, and the reduced transition probability is

$$dB(\mathcal{E}1;0^+_{\text{g.s.}}\rightarrow 1^-(E))/dE$$

$$=\int |\langle 1^-(E)||T^{\mathcal{E}}_{1m}||0^+_{\text{g.s.}}\rangle|^2 d\rho_f\,\delta(E_f-E), \qquad (27)$$

with a non-energy-weighted sum rule limit of

$$\int dE\, dB(\mathcal{E}1;0^+_{\text{g.s.}}\rightarrow 1^-(E))/dE=\frac{3}{4\pi}e^2Z_3^2\langle 0^+_{\text{g.s.}}|r_3^2|0^+_{\text{g.s.}}\rangle. \qquad (28)$$

The energy-weighted sum

$$\int dE(E-E_{\text{g.s.}})dB(\mathcal{E}1;0^+_{\text{g.s.}}\rightarrow 1^-(E))/dE \qquad (29)$$

uses a closure integral of the form

$$s_1=\sum_\nu (E_\nu-E_{\text{g.s.}})|\langle \nu|\mathbf{D}|0\rangle|^2=1/2\langle 0|[\mathbf{D},[H,\mathbf{D}]]|0\rangle, \qquad (30)$$

which, inserting the kinetic energy for H and eliminating the c.m. motion, is approximately

$$s_1=3Z_3^2\hbar^2(A_1+A_2)/(2mAA_3). \qquad (31)$$

Thus we get[1]

$$\int dE(E-E_{\text{g.s.}})dB(\mathcal{E}1;0^+_{\text{g.s.}}\rightarrow 1^-(E))/dE$$

$$=\frac{9}{4\pi}\frac{A_1+A_2}{AA_3}\frac{\hbar^2e^2Z_3^2}{2m}. \qquad (32)$$

From the non-energy-weighted rule, we see that the integrated dipole response depends on the core mean square radius within the halo, so models with large halos (e.g., in ^{11}Li from s-intruder states [80,81]) should have enhanced dipole breakup. The ratio of the energy-weighted to the non-energy-weighted sum-rule limits will give a primitive indication of the mean excitation energy of the dipole response.

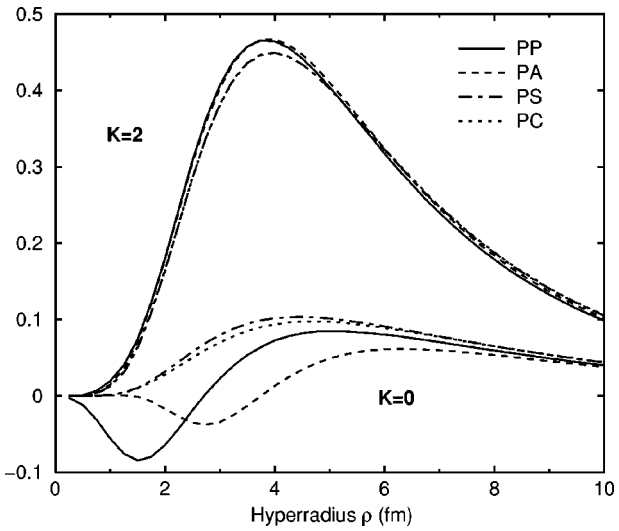

FIG. 1. The $K=0$ and $K=2$ hyperspherical $L=S=l_x=l_y=0$ components of the wave functions of ^{6}He in different Pauli treatments, with potentials adjusted for the same ground state energy.

III. CALCULATIONS FOR ^{6}He

A. Pairwise interactions

For the nn interaction we use a ''realistic'' potential: the Gogny–Pires–de Tourreil (GPT) potential [82]. This includes $\mathbf{l}\cdot\mathbf{s}$ as well as tensor components, and has a soft repulsive core. For the neutron-core (αn) interaction, we use a central Woods-Saxon (WS) of range 2.0 fm and a spin-orbit WS-derivative form, to fit the experimental scattering phase shifts [83] satisfactorily. This WS potential has already been used in the coordinate-space Faddeev calculation [67] for ^{6}Li, and is

$$V_{\alpha n}(r)=\frac{-43.0}{1+\exp[(r-R_{\alpha n})/a]}$$

$$+\frac{\mathbf{l}\cdot\mathbf{s}}{r}\frac{d}{dr}\frac{40.0}{1+\exp[(r-R_{so})/a_{so}]}\ \text{MeV}, \qquad (33)$$

where $R_{\alpha n}=2.0$ fm, $R_{so}=1.5$ fm, $a=0.7$ fm, and $a_{so}=0.35$ fm, although this particular choice is perhaps a little too attractive for d waves. We therefore used the value -21.5 MeV for the d-wave central part and zero for partial waves $l\geqslant 3$.

For this choice of $V_{n\alpha}$, the present calculations take the Pauli exclusion principle into account by the three different methods, as classified above.

PP: Orthogonalizing the three-body wave functions (bound and scattering) to the occupied $0s$ two-body state found as the deeply bound eigenstate ($E=-9.8$ MeV) of the above $V_{n\alpha}$ potential.

PS: Supersymmetric transformation of the attractive s-wave $V_{n\alpha}$ potential gives a purely repulsive partner (see, e.g., Fig. 1 in [62]). This partner shows the same s-wave

[1]In [79] a slightly different expression is given—A_3/A times ours—in accordance with an incomplete elimination of the c.m. motion.

TABLE I. Calculated ground state for ^{6}He using the various Pauli treatments with $K_{max}=20$. For each method, a three-body potential of the strength V_3 shown was needed to reproduce the experimental separation energy of 0.97 MeV. R_m is the matter radius of ^{6}He, using an α matter radius taken as 1.47 fm. The EWSR(1^-) and NEWSR(1^-) values are from Eqs. (32) and (28), respectively, and $\tilde{E}(1^-)$ is the sum-rule estimate of the 1^- excitation centroid relative to the breakup threshold.

Pauli method	V_3 MeV	$E_{g.s.}$ MeV	$\langle\rho^2\rangle^{1/2}$ fm	R_m fm	EWSR(1^-) MeV e^2 fm^2	NEWSR(1^-) e^2 fm^2	$\tilde{E}(1^-)$ MeV
PP	0.0	−0.13	6.02	2.73	4.95	1.810	2.60
	1.6	−0.98	5.34	2.49	4.95	1.364	2.65
PC	0.0	Unbound					
	2.4	−0.98	5.51	2.55	4.95	1.494	2.33
PS	0.0	Unbound					
	2.3	−0.97	5.50	2.55	4.95	1.494	2.33
PA	0.0	Unbound					
	1.9	−0.98	5.39	2.51	4.95	1.350	2.69

phase shift, and has a ''Pauli core'' which excludes from the αn potential the $0s$ state occupied by the α-core neutrons.

PC: The repulsive potential may be approximated [4] by a Gaussian potential of size $b=2.3$ fm and $V_{n\alpha}(l=0)=+50$ MeV, as this also reproduces the experimental $s_{1/2}$ phase shifts [83].

PA: Diagonalize the coupling potential $V_{K'\gamma',K\gamma}(\rho)$ at each hyperradius ρ, and remove the subset of eigensolutions corresponding to eigenvalues of V which are still negative for large ρ. There is such one eigensolution when calculating the 0^+ ground state, and the two lowest solutions for 1^- three-body states, because the $0s_{1/2}$ occupied state can only couple with $s_{1/2}$ to form 0^+, but with both $p_{1/2}$ and $p_{3/2}$ to form 1^- states.

B. Ground state

The three-body method with any of these interactions suffers from the common problem of underbinding [3]. The PP result is the most bound, but still gives a binding energy of $\sim$0.15 MeV instead of 0.97 MeV (see Table I). This underbinding is most likely caused by the influence of other closed channels, most important of which is $t+t$ [16,22,25]. This could be corrected by rescaling the radius or depth of the n-core potentials [3], but here we use an effective three-body potential, giving the same kind of correction as in the three-nucleon system. We shall add to the three-body hyperradial interactions an attractive scalar diagonal three-body potential V_{123} of radius ρ_3, where ρ_3 is chosen as in [9] to be 5 fm:

$$\langle K'\gamma'|V_{123}(\rho)|K\gamma\rangle=-\delta_{K'K}\delta_{\gamma'\gamma}V_3/[1+(\rho/\rho_3)^3]. \tag{34}$$

We calculate with $K_{max}=20$ for the maximum hyperharmonic K used in Eq. (10), and tune the strength V_3 in order to reproduce the experimental three-body separation energy. The results for ^{6}He are shown in Table I. We find that with the PP projection method, a three-body potential of strength $V_3\sim1.6$ MeV needs to be included in order to obtain the correct binding energy. The Pauli treatment methods which use repulsive s-wave potentials, PC and PS, need 2.4 and 2.3 MeV, respectively, whereas the PA method requires 1.9 MeV for the binary interactions selected above. These four interactions gave the weights shown in Table II for the partial components of the wave function in the ground state of ^{6}He. In Fig. 1 we see the $K=0$ and $K=2$ components of the hyperspherical wave functions of ^{6}He in the different Pauli treatments, with potentials adjusted for the same ground-state energy. The dominant $K=2$ wave functions are indistinguishable, whereas the $K=0$ components differ in their nodal behavior at short distances. That from the PP method has a node, in order to have zero overlap with the nodeless occupied $0s_{1/2}$ state. The PC and PS wave functions are nodeless, and pushed out by the repulsive cores. The PA method gives a $K=0$ component with a node, but differs from all the others at short distances. The physical significance of the PA approximation for small hyperradii is not at all transparent.

With local Pauli approximations (PC and PS), the eigenstates obtained are less bound by around 0.5 MeV. This means that we have to increase the three-body potentials up almost 1 MeV, to again fit the observed separation energy. We see that once this is done, somewhat similar characteristics for ^{6}He ground state once more emerge (see also [62]). We argue that since the s wave is anyhow small in the ground-state (g.s.) wave function, it does not appear to matter precisely which method is used to suppress the occupied state.

There is a known 2^+ resonance in ^{6}He at $+1.8$ MeV, so we separately tune V_3 for continuum states, to fit this reso-

TABLE II. Calculated partial-wave percentages for the ^{6}He ground state using different Pauli methods.

Method	$s_{1/2}^2$	$p_{3/2}^2$	$p_{1/2}^2$	$^1S_0$	$^3P_1$
PP	7.7%	85.4%	5.6%	85.3%	11.5%
PC	9.1%	84.7%	4.9%	84.1%	12.3%
PS	9.5%	84.3%	4.9%	84.2%	12.1%
PA	5.8%	87.4%	5.6%	84.8%	12.0%

nance position. We find that the value of V_3 needed here has to be decreased from that to fit the 0^+ ground state, and we use this reduced value for all $J>0$ continuum calculations. For $K_{\max}=20$, we only need 0.90 MeV for the 2^+ resonance in the PP method, so we use this value for the 2^+ state in the PP and PA methods. We need $V_3=0.85$ MeV for the PC method, and we use this for the PC and PS methods in the 2^+ channel.

We have to be careful when introducing a three-body force, however, since it is known that off-shell behavior and three-body forces are tightly connected, one being transformable into the other [84]. Unless we have a very good physical reason for adjusting its strength (such as to fit a resonance position), unnecessary variations of a three-body potential will mask the variations of off-shell behavior that we are trying to probe here. Therefore, for the 1^- channels where there are no defining resonances, we keep $V_3=0.85$ MeV for *all* the Pauli models. This enables the 1^- phase shifts to directly portray the way in which three-body scattering depends on the off-shell features of the two-body subsystems.

With the above adjustments to fit the known g.s. and resonance positions, or lack of adjustments, it will be interesting to compare calculations with deep and repulsive *s*-wave αn interactions, examining in particular the sensitivity of such characteristics as electromagnetic $\mathcal{E}1$ responses and corresponding nuclear responses to the method of exclusion of forbidden states. Some difference should be expected since the internal form of the *s*-wave functions will be different in the two cases: having, for example, different numbers of nodes in the interior, as further discussed below. The three-body results should probe the off-shell properties of the α-nucleon and nn interactions, even in the sparse environment of a nuclear halo.

IV. PAULI EFFECTS IN THE CONTINUUM

Three-body continuum states are a new test bench for the methods mentioned above. The most sensitive indicators are the eigenphases for asymptotic or external properties, which result from the diagonalization of the **S** matrix for the true $3\Rightarrow 3$ resonant scattering and (due to differences in internal structures) the integrated interior norms of the scattering wave functions which show themselves in different reactions.

A. Resonances

The experimentally well-established three-body resonances are the 2^+ state in ^{6}He and the 0^+ ''ground'' state in ^{6}Be, the isospin-multiplet partner of the ^{6}He ground state. Previous calculations [1] with a PC type interaction gave reasonable results for the positions and widths of these states. In Fig. 2 eigenphases and interior norms for ^{6}Be are shown with Coulomb potentials screened at 20 fm and with four variants of the Pauli principle treatment: the PC, PA, PP, and NO PP Pauli treatments. This last calculation uses the deep *s*-wave α-nucleon potential of Eq. (33), without any consideration of forbidden states, and this gives an overbound eigenstate but with approximately the same composition of the wave function. In this last case we have one additional very deep 0^+ three-body bound state below all breakup thresholds, which overlaps almost completely with the two-body occupied states. This deep state should be forbidden in the three-body problem as it would have close to zero norm were a full antisymmetrization operation performed.

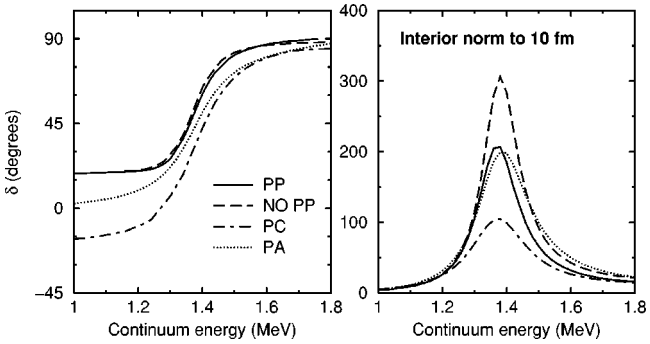

FIG. 2. Eigenphases and interior norms for the 0^+ g.s. of ^{6}Be: PP for Pauli projection, NO PP for no Pauli treatment, PC for repulsive *s*-wave potentials, and PA for adiabatic projections (see text). These calculations use only $K_{\max}=10$.

After adjusting the three-body interactions to put the resonance positions for the ^{6}Be(0^+) ground state close to each other, we can see that these methods give approximately the same shape for the eigenphases dominant in the dynamics of $T=1$ states in $A=6$ nuclei, so the observable widths are similar. The interior norms are, however, different. Physically, projecting out compact forbidden states in the binary subsystems from the three-body Hamiltonian should reduce the three-body wave function in the interior region. This is clearly seen from Fig. 2(b). Simulating the Pauli principle with a repulsive phase-equivalent potential suppresses the wave function in comparison with the PP case. Since the wave functions of the ^{6}Li ground state are normalized to unity, and in both methods the geometrical characteristics of the ^{6}Li g.s. are very close [3], one could hope that the difference of the wave functions could be detected in the magnitude of the charge exchange reaction ^{6}Li$(p,n)^6$Be.

In Fig. 3 the eigenphases and interior norms for the K

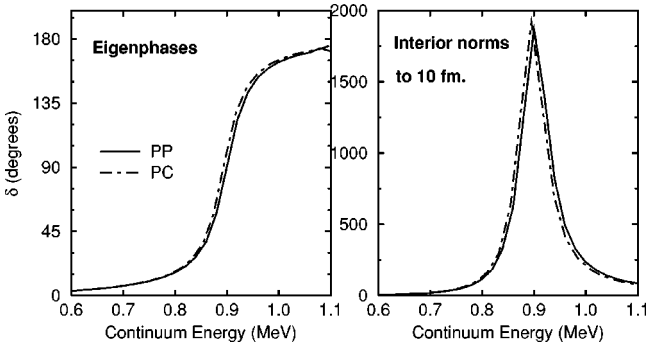

FIG. 3. Eigenphases and interior norms for the $K=2$ channel of the 2^+_1 excited state of ^{6}He. The eigenphases correspond to eigenvectors of the S matrix which are superpositions of all partial waves.

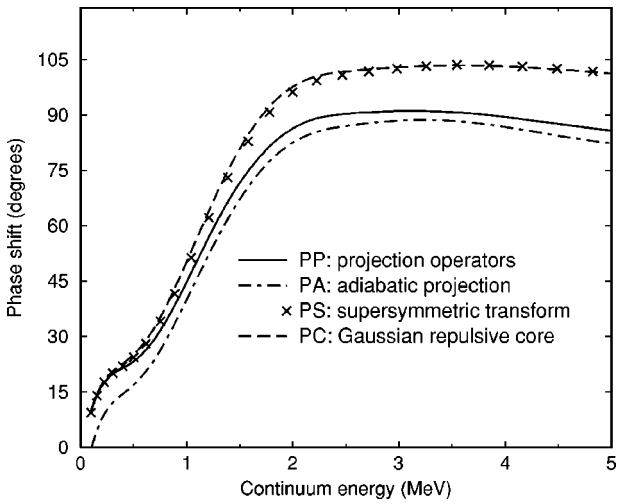

FIG. 4. Diagonal phase shifts for the $K=L=1$, $S=l_x=0$, $l_y=1$ channel in the 1^- continuum, for different Pauli treatments PP, PA, PS, and PC. All curves are from $K_{\max}=20$ calculations with fixed three-body potentials $V_3=0.85$ MeV for the continuum.

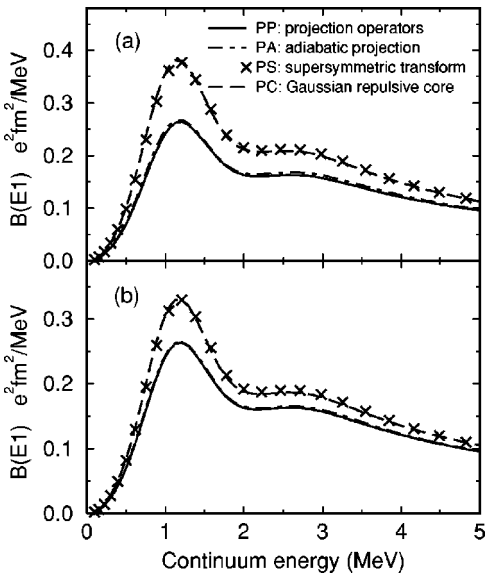

FIG. 5. Dipole $dB(\mathcal{E}1)/dE$ distributions to the 1^- continuum, for different Pauli treatments PP, PA, PS, and PC with $K_{\max}=20$. Curves (a) use g.s. wave functions from the respective methods (with different three-body forces), whereas curves (b) all use the PP g.s. wave function.

$=2$ channel of the 2_1^+ state in ^{6}He are shown for the PC and PP cases, and no differences in the resonant phase and norms are seen. This is expected from angular momentum considerations: the predominant interaction is p wave in the αn subsystems, so a 2^+ state will not feel the s-wave peculiarity.

Summarizing the results for three-body resonances, we can assert that the states with lowest allowed K values are the most sensitive to the off-shell differences of different effective interactions, such as derived from different treatments of the Pauli principle. In, for example, the ^{6}Be 0^+ state, two different treatments of the s-wave αn interaction give the same on-shell behavior, but give different interior norms of the three-body wave function. This is not the case, however, for the first 2^+ state in ^{6}He.

B. Nonresonant continuum

We can also compare the dipole response functions for the different Pauli principle treatments. A 1^- state will consist mostly of $s_{1/2}p_{3/2}$ mixing, while the 0^+ ground state has mainly a $p_{3/2}^2$ combination. The p waves are similar in all cases, but the s waves are different (in the PP case, the s wave should have a node, but not in the PC and PS cases). Thus both theoretical and experimental studies should shed some light on the question of the best treatment of the Pauli principle in three-body systems.

Looking at Fig. 4 we see that the PC and PS phase shifts are practically identical, as well as the PP and PA phases (with the three-body potentials identical in all cases). This implies that changing the precise details of the repulsive (PC or PS) Pauli core does not affect the wave function at large distances, and Fig. 5(a) shows that the corresponding $dB(\mathcal{E}1)/dE$ distributions are the same. These two Pauli-core methods, however, give results which are significantly different from the projection methods PP and PA, as the latter methods give, over most of the low-energy range, *less* positive phase shifts (Fig. 4) and correspondingly less $dB(\mathcal{E}1)/dE$ strength [Fig. 5(a)]. The increase of 46% in the $dB(\mathcal{E}1)/dE$ peak is much larger than the 9% increase to be expected from the change in the non-energy-weighted sum-rule limit shown in Table I, so only part of this increase arises from the changes in the ground-state properties. This is clearly shown in Fig. 5(b), where we artificially use the PP g.s. wave function as the constant initial state for transitions to the continuum in the other Pauli methods. There is evident an increases of 27% in the $dB(\mathcal{E}1)/dE$ peak of the PS and PC methods compared to those of the PP and PA methods.

Because the 1^- continuum states are composed primary from $p_{3/2}\otimes s_{1/2}$ two-neutron configurations, their wave functions in the $s_{1/2}$ channel of neutron-core motion is strongly dependent on the manner of blocking to the bound state in that channel. The large difference between the $dB(\mathcal{E}1)/dE$ predictions of Figs. 5(a) and 5(b) means that experiments might be able to distinguish the PP Pauli principle treatment from the other two (PS and PC). The ground states of $A=6$ nuclei, being dependent only on the ''large'' components of the wave function in channels without forbidden states, are not strongly dependent on the treatment of Pauli blocking.

The $dB(\mathcal{E}1)/dE$ distributions for ^{6}He have recently been obtained [38] at GSI by studies of breakup of ^{6}He on a heavy target. Although the uncertainty limits on the extracted $dB(\mathcal{E}1)/dE$ are quite large (Fig. 4 in [38]), the experimental numbers are distinctly nearer a prediction using the Pauli projection method [9], as this is noticeably less than that using repulsive s-wave potentials [24].

V. CONCLUSIONS

We have performed a thorough investigation of the influence of the Pauli principle treatments on the three-body so-

lutions, and studied the consequences of different treatments having the same two-body on-shell behavior. Summarizing the results, we can assert that for three-body resonances, the states with lowest total K momenta (the lowest configurations in the shell-model language) are most sensitive to off-shell behavior of different effective interactions. As an example, the ^{6}Be 0^+ resonant state, where the s-wave α-n interaction was defined in two ways giving the same on-shell behavior, was found to have a difference in the interior norms of the three-body wave functions. This difference should influence the predicted cross sections in the charge-exchange reaction (^{6}Li,^{6}Be).

The dipole response to the continuum is more sensitive to the Pauli blocking treatment, since it is sensitive to the behavior in the s-wave channel of n-α relative motion. Here, keeping constant three-body potentials, we still see a large difference between the Pauli projection methods and the other more approximate approaches that use repulsive potentials. There are still uncertainties in the exact choice of $n+\alpha$ potentials, but it does appear that the Pauli projection methods give $dB(\mathcal{E}1)/dE$ distributions which are nearer to experiment than those using local l-dependent potentials. The differences are expected to be larger in halo nuclei such as ^{11}Li and ^{14}Be where the s-wave channel plays a significant role even in the ground state [80,12].

ACKNOWLEDGMENTS

B.V.D. thanks the University of Bergen for support for visits, when some of this work was done. B.V.D., M.V.Z., and J.S.V. thank NORDITA for support. U.K. support from EPSRC Grants No. GR/K33026 and GR/L94574, and Russian support from RFBR Grants No. 96-02-17517 and 96-15-96548, is acknowledged. We thank Danas Ridikas for supersymmetric potentials, Torbjoern Rogde for assistance, and Cliff Noble for guidance in R-matrix methods.

[1] B.V. Danilin and M.V. Zhukov, Phys. At. Nucl. **56**, 460 (1993).
[2] M.V. Zhukov, D.V. Fedorov, B.V. Danilin, J.S. Vaagen, and J.M. Bang, Nucl. Phys. **A539**, 177 (1992).
[3] M.V. Zhukov, B.V. Danilin, D.V. Fedorov, J.M. Bang, I.J. Thompson, and J.S. Vaagen, Phys. Rep. **231**, 151 (1993).
[4] B.V. Danilin, M.V. Zhukov, A.A. Korsheninnikov, L.V. Chulkov, and V.D. Efros, Sov. J. Nucl. Phys. **49**, 217 (1989); **49**, 223 (1989); **53**, 45 (1991).
[5] B.V. Danilin, M.V. Zhukov, S.N. Ershov, F.A. Gareev, R.S. Kurmanov, J.S. Vaagen, and J.M. Bang, Phys. Rev. C **43**, 2835 (1991).
[6] B.V. Danilin, M.V. Zhukov, J.S. Vaagen, and J.M. Bang, Phys. Lett. B **302**, 129 (1993).
[7] L.S. Ferreira, E. Maglione, J.M. Bang, I.J. Thompson, B.V. Danilin, M.V. Zhukov, and J.S. Vaagen, Phys. Lett. B **316**, 23 (1993).
[8] B.V. Danilin, T. Rogde, S.N. Ershov, H. Heiberg-Andersen, J.S. Vaagen, I.J. Thompson, and M.V. Zhukov, Phys. Rev. C **55**, R577 (1997).
[9] B.V. Danilin, I.J. Thompson, M.V. Zhukov, and J.S. Vaagen, Nucl. Phys. **A632**, 383 (1998).
[10] S.N. Ershov, T. Rogde, B.V. Danilin, J.S. Vaagen, I.J. Thompson, and F.A. Gareev, Phys. Rev. C **56**, 1483 (1997).
[11] B.V. Danilin, I.J. Thompson, M.V. Zhukov, J.S. Vaagen, and J.M. Bang, Phys. Lett. B **333**, 299 (1994).
[12] I.J. Thompson, B.V. Danilin, V.D. Efros, M.V. Zhukov, and J.S. Vaagen, J. Phys. G **24**, 1505 (1998).
[13] Y. Suzuki, Nucl. Phys. **A528**, 395 (1991).
[14] A. Csótó, Phys. Lett. B **315**, 24 (1993); Phys. Rev. C **48**, 165 (1993); **49**, 3035 (1994); **49**, 2244 (1994).
[15] S. Funada, H. Kameyama, and Y. Sakuragi, Nucl. Phys. **A575**, 93 (1994).
[16] K. Arai, Y. Suzuki, and K. Varga, Phys. Rev. C **51**, 2488 (1995).
[17] S. Aoyama, S. Mukai, K. Kato, and K. Ikeda, Prog. Theor. Phys. **93**, 99 (1995); **94**, 343 (1995).
[18] D.R. Lehman and W.C. Parke, Phys. Rev. C **28**, 364 (1983); **29**, 2319 (1984); **39**, 1685 (1989).
[19] V.I. Kukulin, V.N. Pomerantsev, K.D. Razikov, V.T. Voronchev, and G.G. Ryzhikh, Nucl. Phys. **A586**, 151 (1995).
[20] D. Baye, Y. Suzuki, and P. Descouvemont, Prog. Theor. Phys. **91**, 271 (1994).
[21] E. Garrido, D.V. Fedorov, and A.S. Jensen, Nucl. Phys. **A617**, 153 (1996).
[22] J. Wurzer and H.M. Hofmann, Phys. Rev. C **55**, 688 (1997).
[23] B.S. Pudliner, V.R. Pandharipande, J. Carlson, S.C. Pieper, and R.B. Wiringa, Phys. Rev. C **56**, 1720 (1997).
[24] A. Cobis, D.V. Fedorov, and A.S. Jensen, Phys. Rev. Lett. **79**, 2411 (1997).
[25] K. Arai, Y. Suzuki, and R.G. Lovas, Phys. Rev. C **59**, 1432 (1999).
[26] E. Garrido, D.V. Fedorov, and A.S. Jensen, Nucl. Phys. **A650**, 247 (1999).
[27] A. Eskandarian, D.R. Lehman, and W.C. Parke, Phys. Rev. C **39**, 1685 (1989).
[28] D.V. Fedorov, A.S. Jensen, and K. Riisager, Phys. Rev. C **50**, 2372 (1994).
[29] G.F. Filippov, K. Kato, and S.V. Korennov, Prog. Theor. Phys. **96**, 575 (1996).
[30] A.M. Shirokov, in *Perspectives of Nuclear Physics in the Late Nineties*, Proceedings of the International Conference on Nuclear Physics and Related Topics, Hanoi, Vietnam, 1994, edited by Nguyen Dinh Dang, Da Hsuan Feng, Nguyen Van Giai, and Nguyen Dinh Tu (World Scientific, Singapore, 1995), pp. 295–310; Yu.A. Lurie, A.M. Shirokov, and Yu.F. Smirnov, Rev. Mex. Fis. **40**, Suppl. 1, 63 (1994).
[31] W. Glöckle, H. Witala, D. Hüber, H. Kamada, and J. Golak, Phys. Rep. **274**, 107 (1996).
[32] F. Ajzenberg-Selove, Nucl. Phys. **A490**, 1 (1988).
[33] I. Tanihata, Nucl. Phys. **A522**, 275c (1991).
[34] R. Anne, S.E. Arnell, R. Bimbot, H. Emling, D. Guillemaud-Mueller, P.G. Hansen, L. Johannsen, B. Jonson, M. Lewitowicz, S. Mattsson, A.C. Mueller, R. Neugart, G. Nyman, F.

Pougheon, A. Richter, K. Riisager, M.G. Saint-Laurent, G. Schrieder, O. Sorlin, and K. Wilhelmsen, Phys. Lett. B **250**, 19 (1990).
[35] B. Blank, J.J. Gaimard, H. Geissel, K.H. Schmidt, H. Stelzer, K. Summerer, D. Bazin, R. Del Moral, J.P. Dufour, A. Fleury, H.G. Clere, and M. Steiner, Z. Phys. A **340**, 41 (1991).
[36] K. Ieki *et al.*, Phys. Rev. Lett. **70**, 730 (1993); D. Sackett *et al.*, Phys. Rev. C **48**, 118 (1993).
[37] F. Shimoura *et al.*, Phys. Lett. B **348**, 29 (1995).
[38] T. Aumann *et al.*, Phys. Rev. C **59**, 1252 (1999).
[39] L.V. Chulkov *et al.*, Phys. Rev. Lett. **79**, 201 (1997).
[40] I. Tanihata, T. Kobayashi, O. Yamakawa, S. Shimoura, K. Ekuni, K. Sugimoto, N. Takahashi, T. Shimoda, and H. Sato, Phys. Lett. B **206**, 592 (1988).
[41] T. Kobayashi, Nucl. Phys. **A538**, 343c (1992).
[42] A.A. Korsheninnikov and T. Kobayashi, Nucl. Phys. **A567**, 97 (1994).
[43] D.P. Balamuth *et al.*, Phys. Rev. Lett. **72**, 2355 (1994).
[44] D. Aleksandrov *et al.*, Nucl. Phys. **A633**, 234 (1998).
[45] F. Brady, G.A. Needham, J.L. Romero, C.M. Castaneda, T.D. Ford, J.L. Ullmann, and M.L. Webb, Phys. Rev. Lett. **51**, 1320 (1983).
[46] J. Jänecke *et al.*, Phys. Rev. C **54**, 1070 (1996).
[47] S.B. Sakuta *et al.*, Europhys. Lett. **22**, 511 (1993); **28**, 111 (1994).
[48] Y. Suzuki and Y. Tosaka, Nucl. Phys. **A517**, 599 (1990).
[49] C.A. Bertulani, G. Baur, and M.S. Hussein, Nucl. Phys. **A526**, 751 (1991).
[50] S.A. Fayans, Phys. Lett. B **267**, 443 (1991).
[51] H. Esbensen and G.F. Bertsch, Nucl. Phys. **A542**, 310 (1992).
[52] G. Baur, C.A. Bertulani, and D.M. Kalassa, Nucl. Phys. **A550**, 527 (1992).
[53] J. Bang and C. Gignoux, Nucl. Phys. **A313**, 119 (1979).
[54] Yu.I. Fenin and V.D. Efros, Sov. J. Nucl. Phys. **15**, 497 (1972).
[55] A. Kievsky, M. Viviani, and S. Rosati, Nucl. Phys. **A551**, 241 (1993); **A577**, 511 (1994).
[56] S. Saito, Prog. Theor. Phys. **41**, 705 (1969).
[57] F. Michel and G. Reidemeister, Z. Phys. A **329**, 385 (1988).
[58] D. Baye, Phys. Rev. Lett. **58**, 2738 (1987).
[59] H. Fiedeldey, S.A. Sofianos, A. Papastylianos, K. Amos, and L.J. Allen, Phys. Rev. C **42**, 411 (1990).
[60] Q.K.K. Liu, Nucl. Phys. **A550**, 263 (1992); **A551**, 734 (1993).
[61] D. Ridikas, J.S. Vaagen, and J.M. Bang, Nucl. Phys. **A609**, 21 (1996).
[62] M. Hesse, D. Baye, and J.-M. Sparenberg, Phys. Lett. B **455**, 1 (1999).
[63] R.S. Mackintosh and S.G. Cooper, Nucl. Phys. **A589**, 377 (1995); S.G. Cooper and R.S. Mackintosh, *ibid.* **A592**, 338 (1995).
[64] K. Wildermuth and Y.C. Tang, *A Unified Theory of the Nucleus* (Academic Press, New York, 1977).
[65] J.M. Bang and F.A. Gareev, Nucl. Phys. **A232**, 45 (1974).
[66] R. Courant and D. Hilbert, *Methods of Mathematical Physics* (Interscience, New York, 1953).
[67] J.M. Bang, J.J. Benayoun, C. Gignoux, and I.J. Thompson, Nucl. Phys. **A405**, 126 (1983).
[68] J.M. Bang, in The IMA Volumes of Mathematics and its Applications, *Multiparticle Quantum Scattering With Applications to Nuclear, Atomic and Molecular Physics*, edited by Donald G. Truhlar and Barry Simon (Springer, New York, 1996), Vol. 89, p. 333.
[69] N.W. Schellingerhout, L.P. Kok, S.A. Coon, and R.M. Adam, Phys. Rev. C **48**, 2714 (1993); Phys. Rev. C **52**, 439 (1995).
[70] L.D. Tolsma and G.W. Veltkamp, Comput. Phys. Commun. **40**, 233 (1986).
[71] J.M. Bang, F.A. Gareev, W.J. Pinkston, and J.S. Vaagen, Phys. Rep. **125**, 255 (1985).
[72] F.M. Nunes, I.J. Thompson, and R.C. Johnson, Nucl. Phys. **A596**, 171 (1996).
[73] F.M. Nunes, J.A. Christley, I.J. Thompson, R.C. Johnson, and V.D. Efros, Nucl. Phys. **A609**, 43 (1996).
[74] P.G. Burke and M.J. Seaton, J. Phys. B **17**, L683 (1984).
[75] P.J.A. Buttle, Phys. Rev. **160**, 719 (1967).
[76] V.M. Burke and C.J. Noble, Comput. Phys. Commun. **85**, 471 (1995).
[77] M. Gailitis, J. Phys. B **9**, 843 (1976).
[78] V.V. Pupyshev and S.A. Rakityansky, Z. Phys. A **348**, 227 (1994).
[79] G.F. Bertsch and H. Esbensen, Ann. Phys. (N.Y.) **209**, 327 (1991).
[80] I.J. Thompson and M.V. Zhukov, Phys. Rev. C **49**, 1904 (1994).
[81] J.S. Al-Khalili and J.A. Tostevin, Phys. Rev. Lett. **76**, 3903 (1996).
[82] D. Gogny, P. Pires, and R. de Tourreil, Phys. Lett. **32B**, 591 (1970).
[83] S. Ali, A.A.Z. Ahmad, and N. Ferdous, Rev. Mod. Phys. **57**, 923 (1985).
[84] W.N. Polyzou and W. Glöckle, Few-Body Syst. **9**, 92 (1990).